Organic Cocrystals

Deutsche Ausgabe: DOI: 10.1002/ange.201607712
Internationale Ausgabe: DOI: 10.1002/anie.201607712

Uncovering the Intramolecular Emission and Tuning the Nonlinear Optical Properties of Organic Materials by Cocrystallization

Weigang Zhu, Lingyun Zhu, Lingjie Sun, Yonggang Zhen, Huanli Dong, Zhixiang Wei, and Wenping Hu**

Abstract: *The spectroscopic and photophysical properties of organic materials in the solid-state are widely accepted as a result of their molecular packing structure and intermolecular interactions, such as J- and H-aggregation, charge-transfer (CT), excimer and exciplex. However, in this work, we show that Spe-F$_4$DIB cocrystals (SFCs) surprisingly retain the energy levels of photoluminescence (PL) states of Spe crystals, despite a significantly altered molecular packing structure after cocrystallization. In comparison, Npe-F$_4$DIB cocrystals (NFCs) with new spectroscopic states display different spectra and photophysical behaviors as compared with those of individual component crystals. These may be related to the molecular configuration in crystals, and we propose Spe as an "intramolecular emissive" material, thus providing a new viewpoint on light-emitting species of organic chromophores. Moreover, the nonlinear optical (NLO) properties of Npe and Spe are firstly demonstrated and modulated by cocrystallization. The established "molecule-packing-property" relationship helps to rationally control the optical properties of organic materials through cocrystallization.*

Molecular cocrystals,[1,2] a single-phase material formed with different molecules through non-covalent intermolecular interactions, exhibit unpredicted and versatile chemicophysical properties, such as high conductivity,[3] nonlinear optics (NLO),[4,5] ambipolar charge transportation,[6] ferroelectricity,[7,8] light-driven actuator,[9] and room-temperature phosphorescence.[10] In this context, cocrystallization actually provides an ideal research platform for achieving multiple functions and exploring interesting phenomena in molecular solids. However, a long-standing problem remained in this research field, since the discovery of the first cocrystal quinhydrone in 1844,[11] is how to rationally choose the constituted materials for efficient cocrystallization[12] and desired functions.[13] This requires clear knowledge on i) how different molecules recognize each other, aggregate, nucleate, and grow,[14,15] as well as ii) how molecules and their stacking forms intrinsically affect the resulting bulk properties. Up to now, only a poor understanding of these features has been developed.[16,17] Fortunately, halogen bonding (discovered in 1863)[18] with strong $n \rightarrow \sigma^*$ interactions and excellent directionality[19] has recently been introduced into solid-state reactivity and cocrystallization (superior to other supramolecular interactions),[20,21] which distinctly opens a door for chemists and material scientists to uncover the fantastic phenomena in multi-component molecular solids.[2,10,22] Research on halogen-bonded systems have focused on crystal engineering[22] rather than optoelectronics in the past decades.[23,24] This may be due to the limited experiences for explaining the interesting but complex changes of properties after cocrystallization[16,25] and unclear structure–property relationship in the reported cocrystals,[13,26] particularly for the photophysical and NLO properties.[27,28] These hinder further rational design and preparation of optoelectronic functional halogen-bonded cocrystals. Therefore, the optoelectronic characteristics of halogen-bonded solids and their molecule-packing-property relationship currently remain unknown.

Herein, 4-(1-Naphthylvinyl)pyridine (Npe) and 4-styrylpyridine (Spe) were selected for their unique π-conjugated system and strong halogen-bonding with 1,4-diiodotetrafluorobenzene (F$_4$DIB; Figure 1a). Two new cocrystals were prepared, followed by an in-depth investigation and comparison of their crystal structure, self-assembly, spectroscopic, photophysical, and NLO properties. We show the intrinsic photoluminescence (PL) energy levels of molecules can be changed or retained after cocrystallization, which may be related to the molecular configuration. We present that cocrystallization provides an alternative approach to rationally tune the NLO properties of molecules. Impressively, the molecule-packing-property relationship in this contribution paves the way for further design and preparation of functional cocrystal materials.

Npe and F$_4$DIB molecules in NFC are brought together by C−I⋯N halogen bonds (2.815 Å) and four types of C-F⋯H interactions (Figure S1a,b) to form two-dimensional (2D) molecular planes (Figure 1b), which later pack alternatively along the *a* axis through π-π (donor–acceptor, D-A) interactions (3.372 Å, Figure S1c, d), leading to mixed molecular

---

[*] Dr. W. G. Zhu, Dr. Y. G. Zhen, Dr. H. L. Dong, Prof. W. P. Hu
Institute of Chemistry, Chinese Academy of Sciences (ICCAS)
Beijing 100190 (China)
E-mail: dhl522@iccas.ac.cn
huwp@iccas.ac.cn

Dr. L. Y. Zhu, Prof. Z. X. Wei
National Center for Nanoscience and Technology
Beijing 100190 (China)

Dr. W. G. Zhu
University of Chinese Academy of Sciences
Beijing 100049 (China)

L. J. Sun, Prof. W. P. Hu
Tianjin Key Laboratory of Molecular Optoelectronic Sciences
Department of Chemistry, School of Science
Tianjin University & Collaborative Innovation Center of
Chemical Science and Engineering (Tianjin)
Tianjin 300072 (China)

Supporting information for this article can be found under:
http://dx.doi.org/10.1002/anie.201607712.

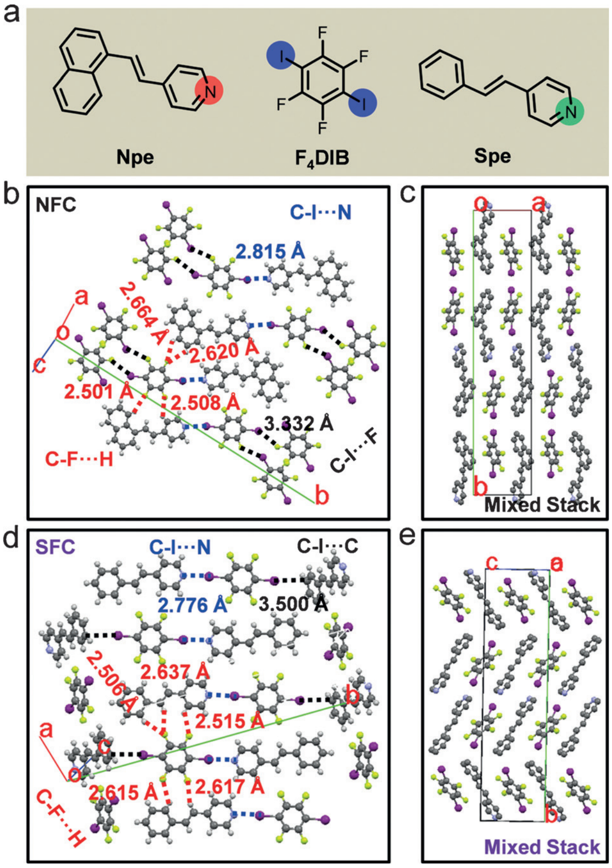

Figure 1. a) Molecular structure of Npe, F_4DIB, and Spe. Intermolecular interactions and molecular packing structures of b, c) NFC and d, e) SFC.

columns (Figure 1 c). Each column then communicates with each other through C−I···F interactions (3.332 Å) to generate the resulting lattice structure. Similarly, 2D molecular planes of Spe and F_4DIB in SFC are formed with C−I···N halogen bonds (2.776 Å) and five types of C−F···H interactions (Figure 1 d), and then stack along the *c* axis through π-π (D-A) interactions (3.832 Å, Figure S2) in a mixed fashion to produce molecular columns (Figure 1 e), which are connected by C−I···C interactions (3.500 Å) to form the final architecture. In this way, the molecular packing structures and intermolecular interactions of NFC and SFC are significantly different from those of the single-component crystals (Figure S3).

Morphology predictions were conducted by using the growth morphology algorithm of Materials Studio software.[29] The result indicates Npe and F_4DIB molecules will grow into a rectangle-like crystal with a dominant (020) face (Figure 2 a, S4a), while Spe and F_4DIB molecules may co-assemble into crystal with a largest (020) face (Figure 2 b, S4b). Cocrystals were prepared by solution drop-casting. The optical images (Figure 2 c,d) confirm that the obtained NFCs show the same morphology as the calculation results, while SFCs exhibit a parallelogram-like shape, both of which are largely different from those of single-component crystals (Figure S5–S7). The transmission electron microscopy (TEM) and selected area electron diffraction (SAED) images of individual NFC (Figure 2 e) and SFC (Figure 2 f) illustrate their single-crystalline nature. NFC belongs to the monoclinic space group $P2_1/c$ with cell parameters of $a = 8.13$ Å, $b = 39.86$ Å, $c = 6.40$ Å, $\alpha = \gamma = 90°$, $\beta = 93.60°$ (Table S1), while SFC belongs to $P2_1/n$ with cell parameters of $a = 6.36$ Å, $b = 33.48$ Å, $c = 9.09$ Å, $\alpha = \gamma = 90°$, $\beta = 110.02°$ (Table S2). Thus, the SAED pattern of NFC with measured *d*-spacing values of 8.04 Å, 6.47 Å and intersection angle 93° can be assigned to (100) and (001), respectively. This was also confirmed by the X-ray diffraction (XRD) result, in which strong (0n0) peaks were observed (Figure S8a, S9a). And the SAED image of SFC with intersection angle of 110° can be attributed to [100] and [001] directions, respectively, which was further verified by the XRD measurements (Figure S8b, S9b,c). The morphology and structure results of the two cocrystals are in accordance with the predictions. Moreover, the cocrystal nature of NFCs and SFCs was further confirmed with comprehensive investigations of their intermolecular interactions and anisotropic properties (Figure S10–S14).

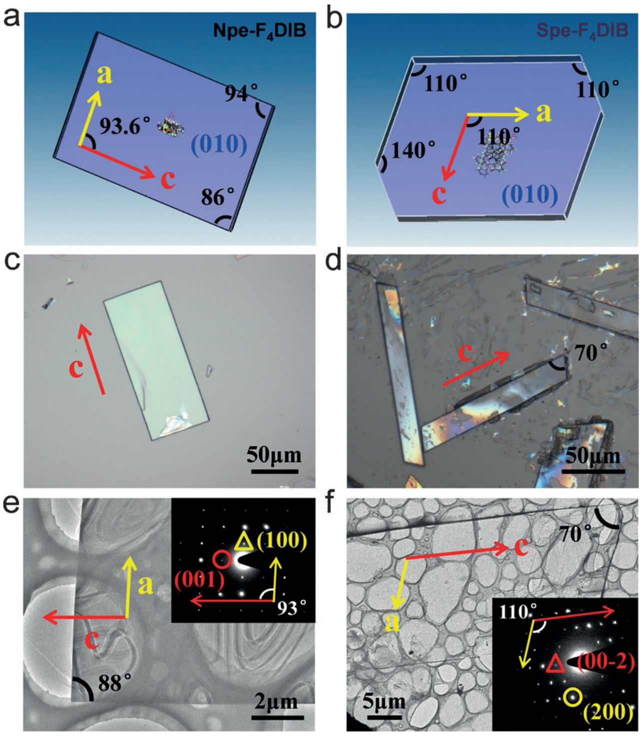

Figure 2. The predicted growth morphology of a) NFC and b) SFC. The optical images of c) NFC and d) SFC on the glass substrate. The typical TEM and SAED images of individual e) NFC and f) SFC.

Figure 3 and Table S3 show the photophysical properties. The confocal laser scanning microscope (CLSM) images of two cocrystals (Figure 3 a,b) clearly illustrate their blue PL and excellent self-waveguide properties (Figure S15). The absorption and PL spectra of NFCs are red-shifted and significantly changed compared with those of individual component crystals (Figure 3 c, S16–S18), while SFCs surprisingly display nearly identical absorption and PL spectra to those of Spe crystals. To our knowledge, the unique spectroscopic behavior of SFCs and Spe crystals here is confusing, because the molecular packing structure is greatly changed

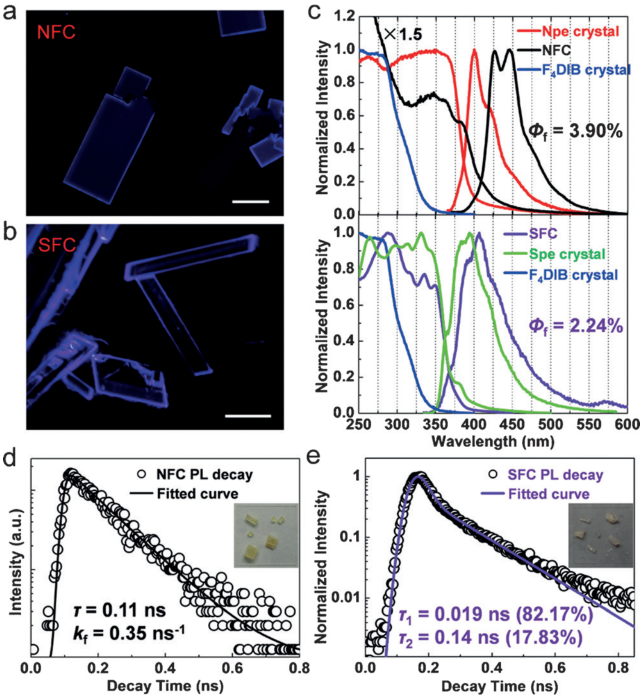

Figure 3. The CLSM images of a) NFCs and b) SFCs. The scale bars are 50 μm. c) The absorption and PL spectra of crystals. The typical PL decay profile of d) NFC and e) SFC. Inserts are the crystals for measurements.

after cocrystallization (from "herringbone packing" in Spe crystal to "mixed stacking" in SFC), which was regarded as an advanced approach to tune the optical properties of organic materials.[13,16,25] To reveal this interesting phenomenon, time-resolved PL measurements were conducted. For Npe crystals (Figure S19d–f), well-structured PL from the lowest locally excited (LE) state (S_1) with monomeric $\tau = 1.55$ ns and $k_f = 0.1\ \text{ns}^{-1}$, indicates that the intramolecular charge-transfer (ICT) in the ground state is destroyed and no photo-induced ICT is happened, which is attributed to the fact that Npe molecules in crystal are twisted and limited by the lattice.[30] The structural rigidification and AIEE effect[31] is thereby triggered and photoluminescence quantum yield (PLQY, Φ_f) is largely enhanced (from 2.30 % to 15.52 %). After cocrystallization, NFCs with red-shifted, distinct absorption and PL spectra display $\Phi_f = 3.90\,\%$, $\tau = 0.11$ ns, $k_f = 0.35\ \text{ns}^{-1}$ (Figure 3d), and the mono-exponential lifetime implies that the PL of NFCs is from one excited state without other competing radiative deactivation processes. These allow us to propose that new spectroscopic states with different energy levels in NFCs are generated (Figure S21c), thus leading to the observed significantly different spectroscopic and photophysical properties from Npe crystals. The $\lambda = 386$, 365 and 345 nm absorption peaks of NFCs (Figure S16c) are assigned to the 0–0, 0–1, and 0–2 transitions to the S_1 state, respectively, and the well-structured PL peaks of NFCs $\lambda = 425$, 445, and 480 nm are attributed to the 0–0, 0–1, and 0–2 transitions from the S_1 to S_0 state. Furthermore, the absorption spectra of Npe, F_4DIB, and Npe-F_4DIB were simulated and assigned (Figure S22–S24).

For Spe crystals, the ground state is neutral without ICT, whereas the PL is contributed from both of S_1 ($\tau_1 = 0.11$ ns, 82.14 %) and ICT ($\tau_2 = 0.77$ ns, 17.86 %) excited states (Figure S25c–e, S26, S27). Owing to the forbidden nature of transition from the S_0 to ICT state, the corresponding oscillator strength (f) of $\lambda = 382$ nm (3.25 eV) absorption is very small. The time-resolved PL spectra of Spe crystals (Figures S29, S30a–c) also demonstrate the existence of short-lived high-energy LE species and long-lived low-energy ICT species (3.23 eV). For SFCs, the Φ_f is 2.24 % (Figure 3c) and the corresponding PL lifetime (Figure 3e) is fitted as double-exponential values of $\tau_1 = 0.019$ ns (82.17 %) and $\tau_2 = 0.14$ ns (17.83 %) with the same percent (Table S3). The time-resolved PL results of SFCs (Figures S30d–f, S31) show that the spectra of short- and long-lived excited species are almost the same as those of Spe crystals. These imply that the energy levels of excited PL states of SFCs do not change as compared with Spe crystals (Figure S21d). The observed absorptions of SFCs are attributed (Figure S21b, d), while the PL is similarly arising from S_1 and ICT states with largely lowered τ and Φ_f, because the introduction of F_4DIB increases non-radiation ways from the corresponding PL states. Moreover, examining the absorption spectra of Spe crystal and SFC carefully, high energy peaks are quite different (Figure S16), and the $\lambda = 382$ nm peak of Spe crystals disappears after cocrystallization. This is because the electronic transition from the S_0 to ICT state in SFC is completely forbidden (Figure S21 d) as a result of molecular packing structures (Figure S32).

The different photophysical phenomena in two cocrystals may be intrinsically related to the molecular configuration in crystals. Npe is changed from twisted in Npe crystal to planar in NFC, while the Spe molecules in SFC retain the planar configuration as that in Spe crystal (Figure S21e). In this sense, the PL spectra of Spe molecules in the solid state surprisingly seem to be not related to their molecular packing structure, surrounding molecular environments, intermolecular interactions, or crystalline quality (Figure S27). We thereby classify this kind of organic light-emitting category as an "intramolecular emissive" material,[23] which means that the PL spectrum of molecules in the solid state cannot be influenced by molecular stacking and intermolecular interactions (like dimers[32] or aggregates[33,34]). Cocrystallization here becomes a powerful tool to reveal the intrinsic luminescent properties of molecules.

Finally, the NLO properties were investigated. The up-conversion PL spectra of Npe crystal excited with $\lambda = 720$ nm laser (Figure 4a) are found to be the same as the steady one, but the f of the 0–0 peak is lowered due to self-absorption. Increasing the power of excitation laser, the recorded PL intensity ($\lambda = 420$ nm) of Npe crystal is increased, showing a fitted linear relation (Figure 4b), which exactly confirms the TPA process.[16] Efficient TPA is also confirmed when the excitation wavelength $\lambda_{ex} = 720$–780 nm (Figure S33, Table S4). Npe crystal with P-1 space group showing TPA property agrees well with the typical D-π-A model.[4,35,36] Similarly, NFC displays TPA property when $\lambda_{ex} = 720$–840 nm (Figures 4c,d, S34) and the up-conversion PL spectra are the same as its steady one. The origin of TPA in NFC might be related to the supramolecular electronic polariza-

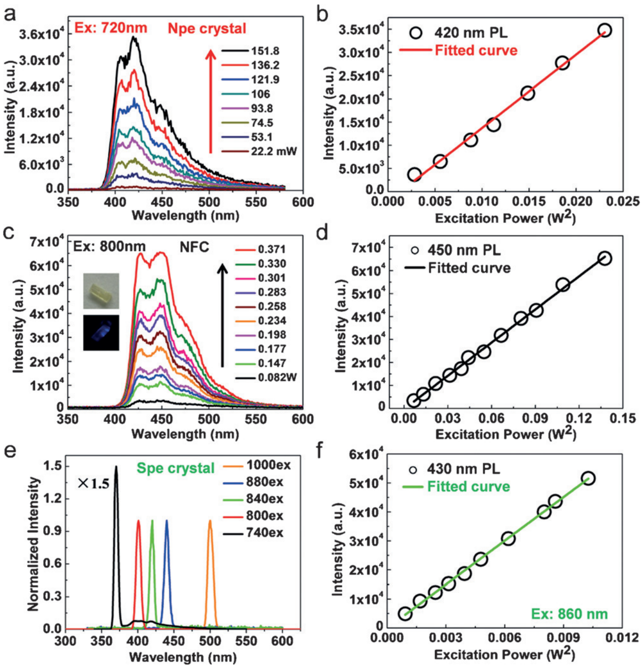

Figure 4. a) The up-conversion PL spectra of Npe crystal and b) corresponding linear relation between the PL intensity and excitation power (W^2). c) The collected PL spectra of NFC under $\lambda = 800$ nm laser excitation, and d) a linear relation is fitted. e) The up-conversion PL spectra of Spe crystal and f) typical linear relation, clearly exhibiting SHG effect.

tion,[4] in which the halogen-bonding acts as a bridge to connect the π-conjugated systems of Npe and F_4DIB, leading to the expansion of the D-π-A configuration. Surprisingly, Spe crystals show SHG properties when $\lambda_{ex} = 740$–1000 nm (Figure 4e, Table S4). A sharp peak at 370 nm with relative weak PL (from re-absorption of the 370 nm light) similar to the steady one is observed when Spe crystal is under the $\lambda =$ 740 nm excitation. Typically, the intensity of the sharp PL peak ($\lambda = 430$ nm) and excitation laser power (W^2, $\lambda =$ 860 nm) are also fitted as a linear relation (Figures 4f, S35). The Spe crystal exhibits SHG properties owing to the D-A configuration of Spe molecule with intramolecular electronic polarization[37] and its non-centrosymmetric Pa crystal space group.[37,38] However, SFCs with low Φ_f do not show any SHG or TPA properties. Spe-F_4DIB halogen-bonded D-π-A system with supramolecular electronic polarization packs as centrosymmetric $P2_1/n$ crystal space group, leading to the suppression of SHG effect.[38] Here, the NLO properties of Npe and Spe are first demonstrated and tuned by cocrystallization.

In conclusion, two new halogen-bonded cocrystals have been prepared, and their crystal structure, intermolecular interactions, morphology, and self-assembling behavior, as well as spectroscopic, photophysical, and NLO properties are compared. We demonstrate that the energy levels of PL states of organic molecules can be changed or retained by cocrystallization, and these may be related to the molecular configuration in crystals, which leads us to propose Spe as an intramolecular emissive material. Cocrystallization is also shown as an alternative approach to tune the NLO properties of organic materials. Significantly, the molecule-packing-property relationship described here is helpful in the rational design and preparation of cocrystals with desired properties.

Acknowledgements

We sincerely acknowledge Dr. Xianzi Dong and Dr. Junfang Zhao (TIPC, CAS) for the help with NLO characterizations, Dr. Mingxing Chen (Peking University) for the help with PLQY and PL lifetime measurements, Dr. Yishi Wu and Prof. Hongbing Fu (ICCAS) for the help with time-resolved PL measurements. This work was supported financially by the Ministry of Science and Technology of China (2016YFB04001100, 2013CB933403, 2013CB933504), the National Natural Science Foundation of China (91222203, 91233205, 91433115, 51303185, 21473222), Chinese Academy of Sciences (XDB12030300).

Keywords: cocrystals · density functional theory · nonlinear optics · organic crystals · photophysics

How to cite: *Angew. Chem. Int. Ed.* **2016**, *55*, 14023–14027
Angew. Chem. **2016**, *128*, 14229–14233

---

[1] a) P. Hu, K. Du, F. Wei, H. Jiang, C. Kloc, *Cryst. Growth Des.* **2016**, *16*, 3019–3027; b) S. Aitipamula, et al., *Cryst. Growth Des.* **2012**, *12*, 2147–2152.
[2] a) Y. L. Lei, L. S. Liao, S. T. Lee, *J. Am. Chem. Soc.* **2013**, *135*, 3744–3747; b) W. Zhu, Y. Zhen, H. Dong, H. Fu, W. Hu, *Prog. Chem.* **2014**, *26*, 1292–1306.
[3] L. B. Coleman, M. J. Cohen, D. J. Sandman, F. G. Yamagishi, A. F. Garito, A. J. Heeger, *Solid State Commun.* **1973**, *12*, 1125–1132.
[4] T. Gotoh, K.-i. Kubodera, T. Kondoh, K. Egawa, *J. Opt. Soc. Am. B* **1989**, *6*, 703–706.
[5] S. M. Rao, A. K. Batra, R. B. Lal, R. A. Evans, B. H. Loo, R. M. Metzger, W. J. Lee, *J. Appl. Phys.* **1991**, *70*, 6674–6678.
[6] J. Zhang, J. H. Tan, Z. Y. Ma, W. Xu, G. Y. Zhao, H. Geng, C. A. Di, W. P. Hu, Z. G. Shuai, K. Singh, D. B. Zhu, *J. Am. Chem. Soc.* **2013**, *135*, 558–561.
[7] S. Horiuchi, F. Ishii, R. Kumai, Y. Okimoto, H. Tachibana, N. Nagaosa, Y. Tokura, *Nat. Mater.* **2005**, *4*, 163–166.
[8] A. S. Tayi, A. K. Shveyd, A. C. H. Sue, J. M. Szarko, B. S. Rolczynski, D. Cao, T. J. Kennedy, A. A. Sarjeant, C. L. Stern, W. F. Paxton, W. Wu, S. K. Dey, A. C. Fahrenbach, J. R. Guest, H. Mohseni, L. X. Chen, K. L. Wang, J. F. Stoddart, S. I. Stupp, *Nature* **2012**, *488*, 485–489.
[9] M. Morimoto, M. Irie, *J. Am. Chem. Soc.* **2010**, *132*, 14172–14178.
[10] O. Bolton, K. Lee, H.-J. Kim, K. Y. Lin, J. Kim, *Nat. Chem.* **2011**, *3*, 205–210.
[11] F. Wöhler, *Justus Liebigs Ann. Chem.* **1844**, *51*, 145–163.
[12] C. Aakeröy, *Acta Crystallogr. Sect. B* **2015**, *71*, 387–391.
[13] J. D. Wuest, *Nat. Chem.* **2012**, *4*, 74–75.
[14] K. Lien Nguyen, T. Friscic, G. M. Day, L. F. Gladden, W. Jones, *Nat. Mater.* **2007**, *6*, 206–209.
[15] M. Boterashvili, M. Lahav, S. Shankar, A. Facchetti, M. E. van der Boom, *J. Am. Chem. Soc.* **2014**, *136*, 11926–11929.
[16] D. Yan, A. Delori, G. O. Lloyd, T. Friščić, G. M. Day, W. Jones, J. Lu, M. Wei, D. G. Evans, X. Duan, *Angew. Chem. Int. Ed.* **2011**, *50*, 12483–12486; *Angew. Chem.* **2011**, *123*, 12691–12694.

[17] D. Vermeulen, L. Y. Zhu, K. P. Goetz, P. Hu, H. Jiang, C. S. Day, O. D. Jurchescu, V. Coropceanu, C. Kloc, L. E. McNeil, *J. Phys. Chem. C* **2014**, *118*, 24688 – 24696.

[18] F. Guthrie, *J. Chem. Soc.* **1863**, *16*, 239 – 244.

[19] A. C. B. Lucassen, A. Karton, G. Leitus, L. J. W. Shimon, J. M. L. Martin, M. E. van der Boom, *Cryst. Growth Des.* **2007**, *7*, 386 – 392.

[20] P. Metrangolo, G. Resnati, *Chem. Eur. J.* **2001**, *7*, 2511 – 2519.

[21] A. Crihfield, J. Hartwell, D. Phelps, R. B. Walsh, J. L. Harris, J. F. Payne, W. T. Pennington, T. W. Hanks, *Cryst. Growth Des.* **2003**, *3*, 313 – 320.

[22] H. L. Nguyen, P. N. Horton, M. B. Hursthouse, A. C. Legon, D. W. Bruce, *J. Am. Chem. Soc.* **2004**, *126*, 16 – 17.

[23] W. Zhu, R. Zheng, Y. Zhen, Z. Yu, H. Dong, H. Fu, Q. Shi, W. Hu, *J. Am. Chem. Soc.* **2015**, *137*, 11038 – 11046.

[24] H. Y. Gao, Q. J. Shen, X. R. Zhao, X. Q. Yan, X. Pang, W. J. Jin, *J. Mater. Chem.* **2012**, *22*, 5336 – 5343.

[25] D. Yan, H. Yang, Q. Meng, H. Lin, M. Wei, *Adv. Funct. Mater.* **2014**, *24*, 587 – 594.

[26] K. P. Goetz, D. Vermeulen, M. E. Payne, C. Kloc, L. E. McNeil, O. D. Jurchescu, *J. Mater. Chem. C* **2014**, *2*, 3065 – 3076.

[27] C. Bosshard, M. S. Wong, F. Pan, P. Günter, V. Gramlich, *Adv. Mater.* **1997**, *9*, 554 – 557.

[28] G. Fan, X. Yang, R. Liang, J. Zhao, S. Li, D. Yan, *CrystEngComm* **2016**, *18*, 240 – 249.

[29] L. Kang, H. Fu, X. Cao, Q. Shi, J. Yao, *J. Am. Chem. Soc.* **2011**, *133*, 1895 – 1901.

[30] W. Z. Yuan, X. Y. Shen, H. Zhao, J. W. Y. Lam, L. Tang, P. Lu, C. Wang, Y. Liu, Z. Wang, Q. Zheng, J. Z. Sun, Y. Ma, B. Z. Tang, *J. Phys. Chem. C* **2010**, *114*, 6090 – 6099.

[31] Y. Dong, J. W. Y. Lam, A. Qin, J. Sun, J. Liu, Z. Li, J. Sun, H. H. Y. Sung, I. D. Williams, H. S. Kwok, B. Z. Tang, *Chem. Commun.* **2007**, 3255 – 3257.

[32] D. Weiss, R. Kietzmann, J. Mahrt, B. Tufts, W. Storck, F. Willig, *J. Phys. Chem.* **1992**, *96*, 5320 – 5325.

[33] U. Rösch, S. Yao, R. Wortmann, F. Wurthner, *Angew. Chem. Int. Ed.* **2006**, *45*, 7026 – 7030; *Angew. Chem.* **2006**, *118*, 7184 – 7188.

[34] F. Würthner, T. E. Kaiser, C. R. Saha-Moller, *Angew. Chem. Int. Ed.* **2011**, *50*, 3376 – 3410; *Angew. Chem.* **2011**, *123*, 3436 – 3473.

[35] M. Albota, D. Beljonne, J.-L. Brédas, J. E. Ehrlich, J.-Y. Fu, A. A. Heikal, S. E. Hess, T. Kogej, M. D. Levin, S. R. Marder, D. McCord-Maughon, J. W. Perry, H. Röckel, M. Rumi, G. Subramaniam, W. W. Webb, X.-L. Wu, C. Xu, *Science* **1998**, *281*, 1653 – 1656.

[36] M. T. Beels, I. Biaggio, T. Reekie, M. Chiu, F. Diederich, *Phys. Rev. A* **2015**, *91*, 043818.

[37] J. L. Oudar, D. S. Chemla, *J. Chem. Phys.* **1977**, *66*, 2664 – 2668.

[38] F. Pan, M. S. Wong, V. Gramlich, C. Bosshard, P. Günter, *J. Am. Chem. Soc.* **1996**, *118*, 6315 – 6316.

Received: August 8, 2016
Revised: September 13, 2016